

## Modulation of wave forces on kelp canopies by alongshore currents

Brian Gaylord<sup>1</sup>

Marine Science Institute, University of California, Santa Barbara, California 93106

Mark W. Denny

Hopkins Marine Station of Stanford University, Pacific Grove, California 93950

Mimi A. R. Koehl

Department of Integrative Biology, University of California, Berkeley, California 94720

### Abstract

The predominant view of the canopy-forming kelp's mechanical response to water motion is that they sway passively under waves such that they are only rarely stretched out in flow, which reduces relative fluid velocities and decreases the applied force. Such a view is an appropriate first-order approximation but becomes conceptually problematic in the face of the net surface velocities (Stokes drift) that arise under waves of all but infinitesimal height, since such flows can tug organisms into fully extended positions, allowing forces to act unabated. Focusing on *Nereocystis luetkeana*, the bull kelp, this study examines quantitatively the capacity of alongshore currents to mitigate the consequences of Stokes drift by maintaining canopy-forming macroalgae in "neutral" positions with regard to the onshore-offshore orbits of the waves. Results indicate that alongshore currents can indeed substantially reduce the forces imposed on canopy-forming kelps, as well as decrease the levels of wave damping that result from the interaction of these organisms with the passing fluid.

Kelp forests provide essential habitat and food for hundreds of species of marine invertebrates and fish living in temperate nearshore waters (Foster and Schiel 1985). The forests' proximity to the shore also makes them vulnerable to hydrodynamic forces imposed by surface gravity waves as these waves shoal into shallow water. Indeed, particularly during severe winter storms, large numbers of canopy-forming macroalgae such as *Macrocystis pyrifera* and *Nereocystis luetkeana* can be dislodged or destroyed by high-amplitude seas and swell (e.g., Seymour et al. 1989; Dayton et al. 1992). The ecological importance of these organisms, and their susceptibility to flow-driven disturbance in the face of a changing wave climate (Bacon and Carter 1991; Greve-meyer et al. 2000), suggests that efforts to understand the plants' mechanical relationship to water motion are both valuable and timely.

The traditional view of the behavior of canopy-forming kelps in flow has been that they move passively with the fluid over substantial portions of each oscillatory wave cycle (i.e., they "go with the flow"), which results in a decrease in the speed of water relative to their fronds, thereby minimizing drag (Koehl 1984, 1986, 1999). In this scenario, it is only the most exceptional wave conditions that result in

the imposition of dangerous forces (in nonwavy habitats, rapid tidal currents can also combine with accumulated grazer damage to cause significant mortality; in other cases, entanglements with already-dislodged individuals may be important [Koehl and Wainwright 1977; Dayton et al. 1992]). This general perspective is supported by observations of seaweed motion in nature (e.g., Koehl 1984), correlative patterns where kelp blades exhibit "slow-flow" morphologies even in moderately wavy locations (Koehl and Alberte 1988; Johnson and Koehl 1994), and a limited number of direct measurements of hydrodynamic forces acting on real organisms in the field (Denny et al. 1997; Gaylord and Denny 1997; Koehl 1999). Complementary flow data gathered using moored instruments also indicate that surface gravity waves are not noticeably damped in passing through kelp forests, which further supports this concept (Elwany et al. 1995).

However, simple dynamical models also suggest that, under certain conditions, large plants can acquire sufficient momentum and can translate far enough that they reach the limits of their range of motion, removing any slack in their stipes. Under such circumstances, decelerating individuals may impart on themselves an "inertial force" as they are jerked to a halt (Denny et al. 1997, 1998; Gaylord and Denny 1997; Gaylord et al. 2001; see also Mendez et al. 1999). At times, these inertial forces are predicted to outweigh the benefits of moving with the fluid. In addition, because such forces are of quite brief duration, they do not necessarily result in a large loss of wave energy and so can remain undetected in force-proxy indicators, such as wave damping estimates.

Such uncertainties in ascertaining the magnitudes of force imposed on canopy-forming kelps are further exacerbated by additional, subtler features of wave-driven water motion. In

<sup>1</sup> Corresponding author (gaylord@lifesci.ucsb.edu).

### Acknowledgments

M. A. McManus and P. Drake generously supplied the nearshore current measurements. We also thank M. A. Palmer and two anonymous reviewers for helpful comments. This is contribution 100 of the Partnership for Interdisciplinary Studies of Coastal Oceans (PISCO): A Long-Term Ecological Consortium funded by the David and Lucille Packard Foundation. Funds were also provided by the National Science Foundation, grants OCE9313891 and OCE9985946 to M.W.D. and OCE9907120 to M.A.R.K.

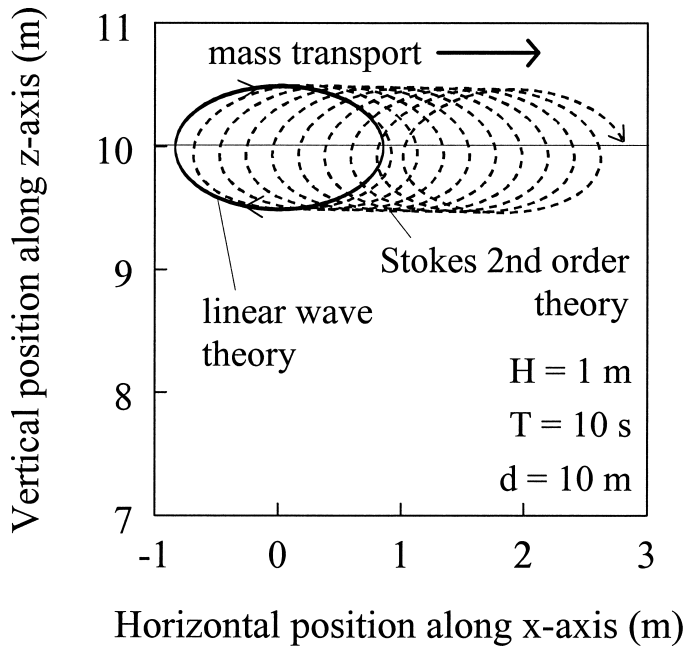


Fig. 1. Net “Stokes drift” under waves of finite amplitude. Higher order corrections (dashed line) to the linear theory (solid line) quantify this near-surface mass transport.  $H$  = wave height,  $T$  = wave period,  $d$  = water depth.

particular, larger-amplitude waves are not fully linear and can induce a net mass transport (Stokes drift) that has the potential to stretch plants out in the direction of wave propagation (Fig. 1; Kinsman 1965; Denny 1988). This drift might be expected to offset the ability of canopy-forming kelps to move continuously with the fluid and could, therefore, substantially increase typical forces (Denny and Gaylord 2002). This in turn could lead to elevated levels of wave damping as well as higher rates of disturbance.

Other, analogous processes might also influence plant dynamics. For instance, local winds blowing in the direction of wave propagation can stretch plants out in much the same way as Stokes drift. Seymour et al. (1989) suggest that this phenomenon might have contributed to the exceptionally high rates of kelp disturbance observed along the coast of Southern California during a 1988 storm. In other cases, alongshore currents (e.g., Jackson and Winant 1983; Jackson 1998) might play a particularly critical role. Such currents tend to flow perpendicular to the waves since waves refract in shallow water to approach almost directly toward a coast. This sets up a scenario where an alongshore current could rotate plants such that they are extended parallel to the shore where they remain in neutral, slack positions with regard to the onshore–offshore orbits of the waves. This could potentially offset the tendency for Stokes drift or an onshore wind to tug organisms into positions where they must cope with the more rapid wave-driven fluid motions. For the same reason, it could influence the amount of wave damping by a kelp forest.

Unfortunately, the consequences of Stokes drift for increasing forces on kelp canopies and for modifying levels of wave damping have not been explored in a rigorous fash-

ion, and the potential mitigating role of alongshore currents has also been ignored. This study therefore attempts a first look at these issues. It focuses on a particular example, *Nereocystis luetkeana*, the dominant canopy-forming kelp along much of the northern portion of the west coast of North America. Although somewhat different morphologically from *Macrocystis pyrifera* (the well-known species forming the massive kelp beds off the coast of Southern California; Dayton et al. 1984) or *Pelagophycus porra* (the so-called “elk kelp”), the dynamics of *Nereocystis* are expected to be at least crudely representative of many surface canopy-forming seaweeds (see below). Numerical experiments are therefore employed to examine the second-by-second dynamical response of *Nereocystis* individuals subjected to nonlinear waves and alongshore currents. This overall approach incorporates a three-dimensional extension to the two-dimensional dynamical kelp model of Denny et al. (1997), which is itself built around extensive macroalgal morphological measurements and empirically determined hydrodynamic parameters. Results indicate that both Stokes drift and alongshore currents can indeed influence the forces imposed on canopy-forming kelps, as well as the level of wave damping that occurs within more extensive beds of these organisms.

### Kelp dynamics

*Nereocystis luetkeana* is a subtidal brown alga of the Order Laminariales that grows with a long, ropelike stipe that extends from the seafloor to the water surface (Abbott and Hollenberg 1976; Koehl and Wainwright 1977). At the distal end of the stipe, an enlarged buoyant float (a pneumatocyst) supports 30–60 ribbonlike blades that together form the kelp’s canopy. The stipes of these organisms typically grow to lengths approximately equal to the water depth, commonly 10 m, which is the value employed for the present study.

A suite of external forces can be imposed in a distributed fashion over the length of any given individual. However, because the bulk of the mass of a *Nereocystis* is located at the distal end of the stipe, the summed effects of these forces can be approximated as if they all act on a point element of equivalent total mass to the whole frond, positioned at the site of the pneumatocyst. There are five external forces of note. The following description of each represents a brief summary of more detailed derivations in Gaylord and Denny (1997) and Denny et al. (1997).

The net buoyant force,  $F_b$ , is the difference between hydrostatic buoyancy and the weight of the organism and is positive upward. In *Nereocystis*, this force arises primarily from the kelp’s pneumatocyst. When the plant’s mass is completely below the water surface,  $F_b$  equals  $F_{sb}$ , its fully submerged value. However, if the pneumatocyst and blades begin to emerge from the water, as can occur in the trough of a wave, the net buoyancy decreases and is approximated by

$$F_b = F_{sb} \left( 1 - \frac{z - [d + \eta]}{0.75} \right) \quad (1)$$

where  $z$  is the height of the plant’s frond mass above the seafloor and  $\eta$  is the sea surface elevation relative to the

mean water depth,  $d$ , all measured in meters. The scaling factor (0.75) in the denominator accounts for the finite dimensions of the pneumatocyst and blades, which precludes an instantaneous exit of the full frond mass from the water. The magnitude of the scaling factor is based on observations of how far real plants in nature extend above the water surface during calm conditions on low tides. Note that all bold-face quantities are vectors.

Drag,  $\mathbf{F}_d$ , results from water moving with respect to a kelp and applies a force in the direction of relative velocity,

$$\mathbf{F}_d = \frac{1}{2} \rho A S_d \mathbf{u}_r u_r^{\gamma-1} \quad (2)$$

where  $\rho$  is the density of seawater,  $A$  is the maximum projected blade area,  $S_d$  is a shape coefficient of drag,  $\gamma$  is a velocity exponent, and  $\mathbf{u}_r$  is the relative velocity. Equation 2 is an equivalent, alternative form to the conventional velocity-squared expression of the engineering literature and has become standard in the biological arena because of its greater ease in parameterizing the processes of reconfiguration and streamlining (Denny 1995; Gaylord 2000).

Virtual buoyancy,  $\mathbf{F}_{vb}$ , derives from the pressure gradient that accompanies a spatially accelerating flow and points in the down-gradient direction (i.e., the direction of acceleration; Gaylord et al. 1994),

$$\mathbf{F}_{vb} = \rho V \mathbf{a} \quad (3)$$

where  $V$  is the volume of fluid displaced by the frond and  $\mathbf{a}$  is the spatial acceleration of the flow relative to the earth.

An added mass force,  $\mathbf{F}_{am}$ , results from fluid accelerating relative to an organism and acts in the direction of that relative acceleration (Batchelor 1967; Gaylord et al. 1994),

$$\mathbf{F}_{am} = C_a \rho V \mathbf{a}_r \quad (4)$$

where  $C_a$  is an added mass coefficient and  $\mathbf{a}_r$  is the total fluid acceleration relative to the plant.

Tension in the stipe of a seaweed,  $\mathbf{F}_t$ , acts as a restoring force when the stipe is extended. This force is modeled as if the stipe were an elastic, massless rope with material stiffness  $E$ . Thus, tension is zero except when the stipe is stretched beyond its resting length,  $L$ , under which conditions the force is given by

$$\mathbf{F}_t = EA_{xs} \left( \frac{\sqrt{x^2 + y^2 + z^2} - L}{L} \right) \quad (5)$$

where  $(x, y, z)$  indicates the position of plant mass in space, and  $A_{xs}$  is the nominal cross-sectional area of the stipe. A traditional right-handed coordinate system is used in which the  $x$ -axis points toward shore parallel to the direction of wave propagation, and  $z$  increases upward from zero at the seafloor.  $\mathbf{F}_t$  acts along the axis of the stipe and is therefore always directed toward the holdfast located at position  $(0, 0, 0)$ . The model also includes additional measures (as in Denny et al. 1997) for preventing unrealistic passage of the plant's mass into the substratum, but because this issue does not arise for the cases examined in this study, these complexities are not discussed further.

According to Newton's Second Law, the imposition of the forces above causes the kelp's front mass,  $m$ , to accelerate,

Table 1. Morphological and hydrodynamical parameters of a typical, mature *Nereocystis luetkeana* individual. Values are from Denny et al. (1997).

Stipe length (m)	10
Net fully submerged buoyant force (N)	14.89
Total plant mass (kg)	6.10
Blade area (m <sup>2</sup> )	7.82
Nominal stipe cross-sectional area (m <sup>2</sup> )	$1.60 \times 10^{-4}$
Plant volume (m <sup>3</sup> )	$2.05 \times 10^{-2}$
Shape coefficient of drag (m <sup>2-<math>\gamma</math></sup> s <sup><math>\gamma-2</math></sup> )	0.016
Drag exponent	1.6
Added mass coefficient	3.0
Stipe stiffness (N m <sup>-2</sup> )	$1.2 \times 10^7$

$$\mathbf{a}_k = \frac{\mathbf{F}_b + \mathbf{F}_d + \mathbf{F}_{vb} + \mathbf{F}_{am} + \mathbf{F}_t}{m} \quad (6)$$

where  $\mathbf{a}_k$  is its acceleration (thus, even when all flow forces are zero, rapid decelerations can induce a finite  $\mathbf{F}_t$  and thereby an inertial force). Equation 6 is then integrated numerically through time to track the plant's instantaneous velocity and position. In practice, this task is accomplished through the use of a standard fourth-order Runge–Kutta algorithm with adaptive time step (Press et al. 1992). Note that this approach provides a detailed description of a kelp's motion and the instantaneous forces imposed on it through time. That is, the analysis does not simply rely on time-averaged values, which are less relevant for understanding organism damage or dislodgment.

The parameter values used to model a typical mature *Nereocystis* are listed in Table 1. All morphological values are extracted directly from the empirical allometric growth data of Denny et al. (1997), whereas the shape coefficient of drag is derived from measurements on current-swept *Nereocystis* plants by Johnson and Koehl (1994). The drag exponent,  $\gamma$ , is based on measurements conducted on *Macrocystis pyrifera* by Utter and Denny (1996) and on measurements using 12 other, somewhat smaller species of macroalgae by Gaylord (2000), as is the added mass coefficient. Note that although Stevens et al. (2001) suggest that the above drag parameters (which are identical to those originally used by Denny et al. [1997]) potentially underestimate force at slower relative velocities ( $<0.1$  m s<sup>-1</sup>) by about a factor of two, the alternative form they propose appears too small by almost a factor of 10 at relative velocities of 1 m s<sup>-1</sup>, and too small by as much as three orders of magnitude at relative velocities of 2 m s<sup>-1</sup>. This point derives from the observation that even smooth, flat plates aligned exactly with flow have drag coefficients that are several hundred times larger at such flow speeds (Schlichting 1979). Because quite substantial relative flow rates are expected for some wave conditions and at certain phases in any given oscillatory cycle, the original drag expression as employed by Denny et al. (1997)—and as validated in the field (*see below*)—is retained here.

The water velocities and accelerations at the location of the kelp's pneumatocyst (i.e., the fluid motions responsible for the imposition of a major subset of the forces above) are estimated via Stokes second-order wave theory (Sarpkaya and Isaacson 1981). This theory uses a perturbation analysis

to improve accuracy over the more commonly used, and perhaps more familiar, linear approximations (e.g., Kinsman 1965; Denny 1988). Predicted wave-driven horizontal and vertical velocities ( $\mathbf{u}_x$  and  $\mathbf{u}_z$ , respectively) therefore become

$$\mathbf{u}_x = \frac{\pi H}{T} \frac{\cosh(kz)}{\sinh(kd)} \cos(kx - \omega t) + \frac{3}{4} \frac{\pi^2 H^2}{T \lambda} \frac{\cosh(2kz)}{\sinh^4(kd)} \cos(2[kx - \omega t]) \quad (7)$$

$$\mathbf{u}_z = \frac{\pi H}{T} \frac{\sinh(kz)}{\sinh(kd)} \sin(kx - \omega t) + \frac{3}{4} \frac{\pi^2 H^2}{T \lambda} \frac{\sinh(2kz)}{\sinh^4(kd)} \sin(2[kx - \omega t]) \quad (8)$$

where the second term in each expression represents the higher-order correction to the linear solution.  $H$  is the wave height (twice the wave amplitude),  $T$  is the wave period,  $\lambda$  is the wavelength,  $k$  is the wavenumber ( $2\pi/\lambda$ ),  $\omega$  is the wave frequency ( $2\pi/T$ ),  $t$  is time, and  $\sinh$  and  $\cosh$  are the hyperbolic sine and cosine, respectively.  $T$ ,  $\lambda$ , and  $d$  are linked according to the dispersion relation

$$C = \frac{\lambda}{T} = \frac{g}{\omega} \tanh(kd) \quad (9)$$

where  $\tanh$  is the hyperbolic tangent. Fluid accelerations are then just the total derivatives,  $d\mathbf{u}_x/dt$  and  $d\mathbf{u}_z/dt$ , of Eqs. 7 and 8. Monochromatic waves are employed to simplify interpretation of results, and an additional, steady alongshore current,  $\mathbf{u}_y = \mathbf{u}_{\text{current}}$ , acts perpendicular to the oscillatory wave motions.

The use of Stokes theory is important because it provides a means of accounting for the tendency for real waves to induce a net mass transport (i.e., Stokes drift). In contrast to the idealized situation of fully linear waves with infinitesimal amplitude, fluid orbits under waves of finite amplitude are not quite closed. This feature results from the depth attenuation intrinsic to wave-driven flows, which causes fluid particles at the tops of their orbits to move forward slightly faster and for a longer time than they move backward at the bottoms of their orbits. The drift velocity that ensues can be calculated as (Komar 1998)

$$\mathbf{u}_{x \text{ drift}} = \left( \frac{\pi H}{\lambda} \right)^2 \frac{C}{2} \frac{\cosh(2kz)}{\sinh^2(kd)} \quad (10)$$

Note that this velocity is maximal at the water surface, where it can interact with a kelp's pneumatocyst and blades, and decreases rapidly below the surface. Thus, although this Stokes solution makes no allowance for a finite flow near the seafloor (a characteristic of more sophisticated theories; e.g., Longuet-Higgins 1953) and must be viewed as an approximation because of limitations on formal convergence of the second-order theory when applied to exceptionally steep waves (Sarpkaya and Isaacson 1981), the simpler form of Eq. 10 is sufficient for the purposes of this study, where all critical force balances operate high in the water column.

It should also be noted that, because wave-driven flows (either those associated with linear or Stokes waves) impose

forces on a plant, a plant in turn applies forces on the water. This process generally results in a loss of kinetic energy from the fluid. The average rate of energy loss over a wave period is at most

$$P_{\text{loss}} = \frac{1}{T} \int_0^T \mathbf{F}_d \cdot \mathbf{u}_r \, dt \quad (11)$$

When compared to the energy flux associated with the passage of a wave train, this quantity provides a rough indication of the maximum possible level of wave damping caused by the kelp. In theory, it is also conceivable that plants could move in such a way so as to transfer some of their own kinetic energy (gained at the expense of wave energy) back to the water. However, the consequences of this plant-to-fluid kinetic energy exchange are assumed minor and are not explored in any detail here.

### Field validation of the dynamical construct

A fully rigorous test of the above model across a complete range of conditions is not yet available because of the experimental and analytical difficulties that arise when confronting nonlinear waves. However, a preliminary check on the efficacy of the approach is possible for the subset of cases where the degree of nonlinearity is small. Gaylord and Denny (1997) and Denny et al. (1997) have conducted such tests previously, and a further example derived from these efforts is included here for completeness. Readers interested in greater detail should consult Denny et al. (1997).

Validation of the dynamical construct proceeded by mounting a 6.6-m-long *Nereocystis* individual on a force transducer positioned in 6.4 m of water within a small embayment at Hopkins Marine Station in Pacific Grove, California. The tensile force applied to the base of the stipe was recorded at 20 Hz by the transducer, and the subsurface pressure at the seafloor immediately adjacent to the plant was measured simultaneously. The sea surface elevation was then computed from the pressure record by decomposing 4,096-point segments of the time series into their Fourier components, correcting for the frequency-dependent depth attenuation that characterizes surface gravity waves and back-transforming (Kinsman 1965). The first 41 Fourier coefficients were used to define the component waves contributing to this variation in sea surface elevation, and the heights and periods of the waves were inserted into Eqs. 7 and 8 to calculate the corresponding velocity components and their respective phases (i.e., the monochromatic wave train assumption is relaxed here). Note, however, that because the Fourier partitioning of a random sea assumes linearity of the wave field (Kinsman 1965), just the first-order terms of the velocity equations were used. This approximation is appropriate in this context because the sea state during the field measurements was dominated by a 16-s-period swell with a significant wave height of 0.8 m, which is only marginally nonlinear. The overall water motions at the location of the kelp were then estimated by summing all of the individual velocity components, and the summed values were inserted into the model together with the buoyancy term and flow factors involving derivatives of velocity (Eq.

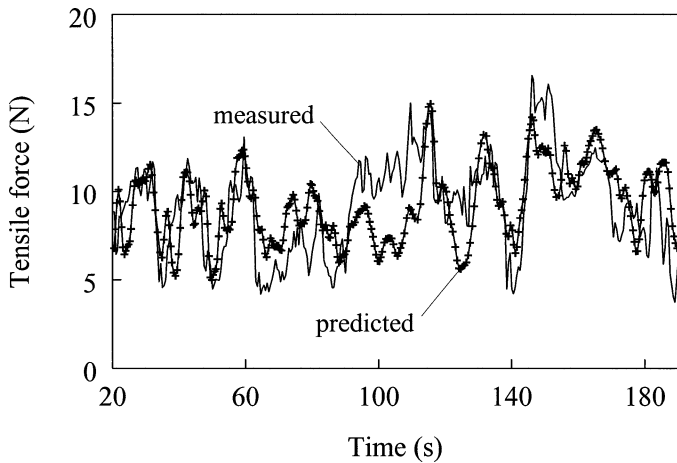


Fig. 2. Example comparison of measured forces imposed on a *Nereocystis* individual in the field (line without symbols), to model predictions (line with crosses).

6) to predict the tensile forces acting on the plant. Finally, the predicted forces were compared, second by second, to the measured forces. As the example data presented in Fig. 2 indicate, although the general modeling approach is highly simplistic, it yields surprisingly accurate descriptions of actual flow forces imposed on kelps in nature.

An additional feature of the field experiments described above provides direct impetus for theoretical components of this study. The narrow embayment used for the force recordings is exposed to surface gravity waves propagating toward shore, but its geometry isolates it almost completely from larger scale alongshore currents. As a consequence, although the lack of alongshore fluid movement simplified the field logistics by eliminating the need to measure steady unidirectional flows (including Stokes drift because of the weak nonlinearity), it also precluded an empirical examination of more complex, three-dimensional motion of kelp individuals subjected simultaneously to both waves and currents. A primary purpose of the model results presented below, therefore, is to explore the consequences of coupled movement along three orthogonal axes at once.

#### Typical wave and current magnitudes

Wave conditions vary tremendously through time even at a single location; thus, kelp beds will generally experience a wide range of sea states. For example, Fig. 3a depicts the mean deep-water wave height spectrum measured offshore of Monterey Bay, California (National Data Buoy Center station 46042; 36°45.183'N, 122°25.350'W), during the winter months of 2001–2002. The error bars representing standard deviations show the high level of variability (which is greatest during this season), a characteristic also seen in plots of significant wave height ( $H_s$ , the average height of the highest one-third waves) measured hourly at the same location over the same duration (Fig. 3b). In general, the recorded dominant wave periods were ~10–12 s (i.e., wave frequencies 0.10–0.08 Hz), but shorter and longer period waves were common (e.g.,  $T \sim 5$ –20 s). Significant wave

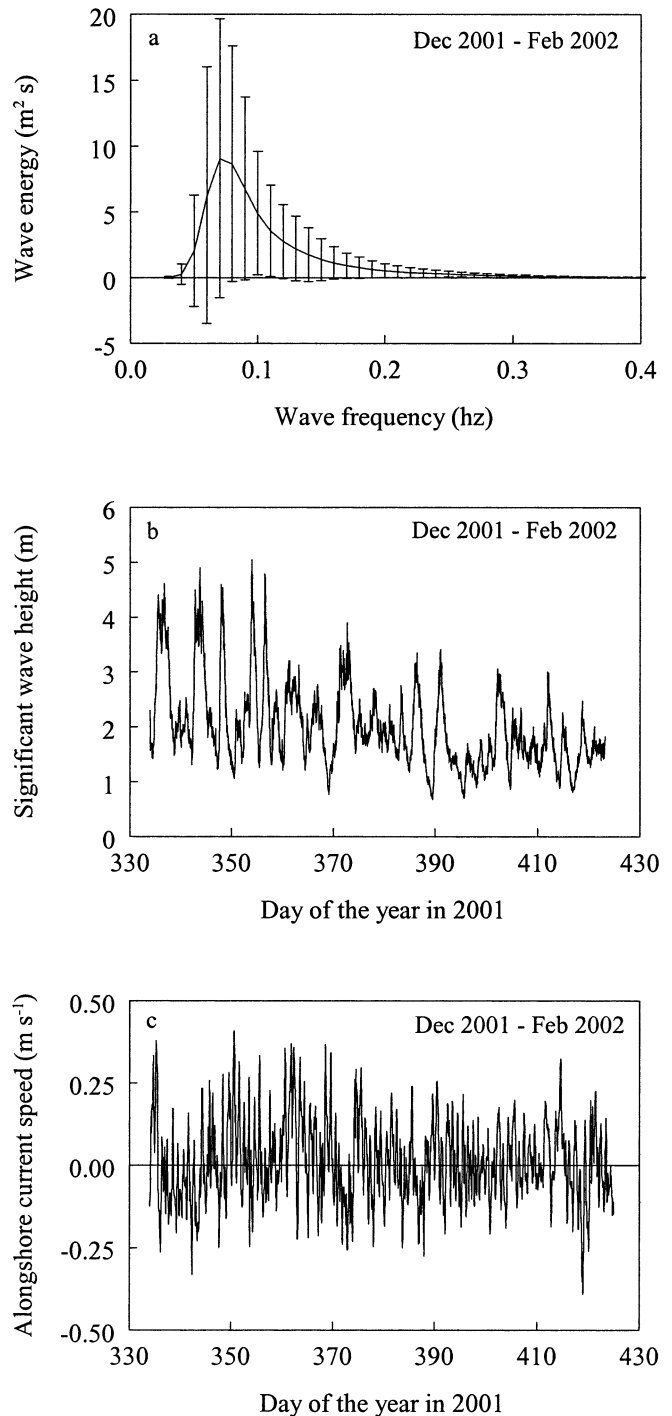


Fig. 3. Wave heights and current speeds in nature. (a) Mean power spectral density curve of wave height recorded just offshore of Monterey Bay, California, during the winter of 2001–2002. Error bars indicate standard deviations of the spectral estimates at each frequency (but note that negative values are nonphysical). (b) Time series of significant wave height for the data of panel a. (c) Time series of near-surface alongshore current magnitudes recorded in 21 m of water just inside Monterey Bay during the winter of 2001–2002. Values along the x-axis showing the day of the year in 2001 are depicted contiguously and therefore exceed 365 as the time sequences enter 2002.

heights in excess of 4 m also occurred routinely. Although it should be noted that the data of Fig. 3a,b represent deep-water wave statistics, and although surface gravity waves do change their height as they shoal into coastal waters, such changes are limited to a few percent until waves approach breaking (Komar 1998). As a result, it can be expected that waves of 1–4 m height and 5–20 s period will impinge on subtidal seaweeds at many central California sites. *Nereocystis* will often avoid the most extreme wave events since (unlike *Macrocystis*) it is essentially an annual species and stops reproducing around December, typically senescing shortly thereafter. However, some *Nereocystis* individuals nonetheless do persist for up to 18 months (Abbott and Hollenberg 1976), making even the more severe wave conditions occasionally relevant.

As might be expected, alongshore current speeds also vary through time. For example, Fig. 3c shows a typical time series of near-surface, alongshore current velocity, averaged hourly, from a site in 21 m of water on the northwest side of Monterey Bay ( $36^{\circ}58.369'N$ ,  $122^{\circ}9.468'W$ ). These measurements were conducted outside, but within a few kilometers of (and in only slightly deeper water than), several local *Nereocystis* beds. As such, the data are roughly indicative of the speeds of currents that impinge on outer margins of kelp beds in this region. An examination of Fig. 3c therefore suggests that at least some plants might encounter alongshore currents as fast as  $0.3\text{--}0.4\text{ m s}^{-1}$ , despite the fact that water movement within beds can be slower because of flow diversion around, and damping within, larger and/or denser forests. Jackson and Winant (1983), for instance, found approximately a threefold reduction in current speed inside the expansive Pt. Loma *Macrocystis* forest off the coast of San Diego, California. The level of flow attenuation within a typical *Nereocystis* bed (which is far smaller than the Pt. Loma forest and where species morphological differences eliminate much midwater plant drag) is likely lower, but a definitive answer to this question awaits further research.

The wave and current data of Fig. 3a–c also span identical durations, which allows for the calculation of rates of co-occurrence of particular wave–current combinations. These rates of co-occurrence are presented in Fig. 4, which shows the fraction of hours during the winter months of 2001–2002 that were characterized by specific combinations of significant wave height, dominant wave period, and alongshore current speed. For example, waves defined by a significant wave height of 0–2 m and a dominant period of 10 s were present together with a  $10\text{ cm s}^{-1}$  alongshore current during approximately 5% (60 h) of the winter (Fig. 4a). Similarly, waves with a significant wave height between 2 and 3 m and a dominant period of 12 s were associated with a current of  $25\text{ cm s}^{-1}$  during approximately 1% (12 h) of the winter (Fig. 4b). Although conditions during other years and months, or at other sites, will obviously differ somewhat from those shown (winter conditions tend to bound those of other seasons), these data provide a general sense of the range of wave–current climates that interact with subtidal macroalgae along substantial portions of the coast of North America.

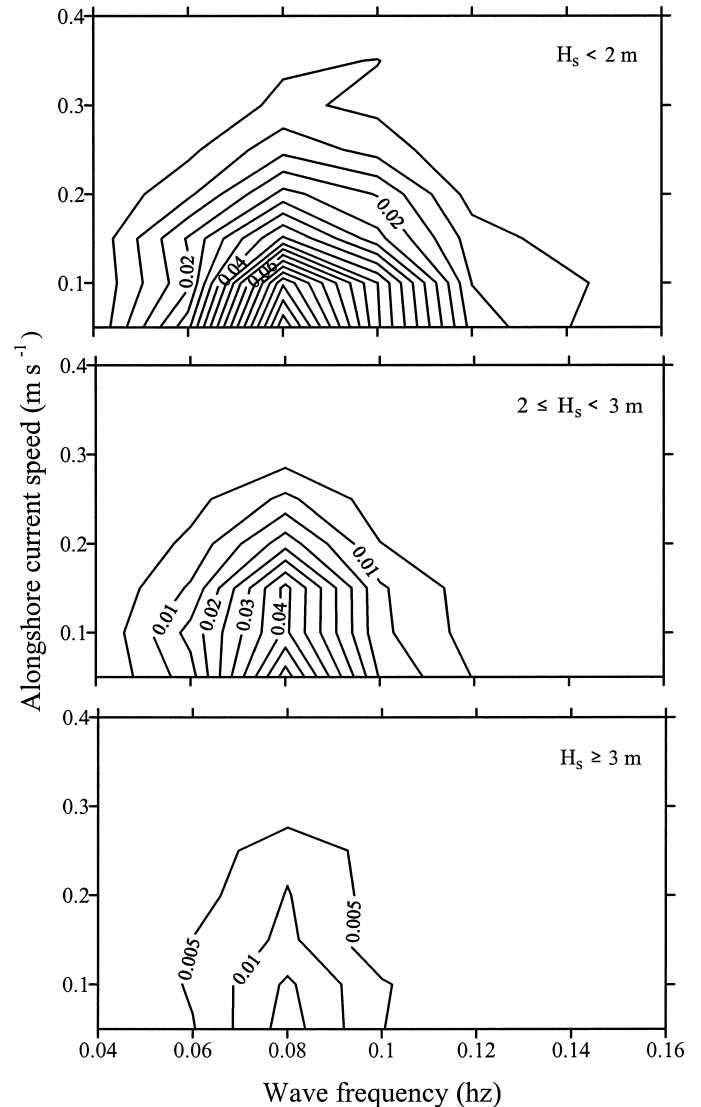


Fig. 4. Rates of co-occurrence of waves and currents. Fraction of hours during the winter of 2001–2002 during which a particular alongshore current velocity occurred in association with a given dominant wave period, when the significant wave height ( $H_s$ ) was (top) 0–2 m, (middle) 2–3 m, or (bottom)  $>3$  m. Contours are smoothed interpolations of bivariate histograms binned at  $0.02\text{ Hz}$  and  $0.05\text{ m s}^{-1}$  increments. The fractional rates of occurrence across all conditions and all three panels integrate to 1.0. Derived from the data of Fig. 3.

#### Predicted forces on canopy-forming kelps and wave damping by them

The above empirical data (i.e., the field measurements of force, wave height, and current speed) have served primarily as validation for the dynamical model and justification for the parameter values employed. With this supporting information in hand, we now turn to a discussion of the model predictions themselves.

As can be seen in Fig. 5, the drift velocities of Eq. 10 induced by finite amplitude waves increase with wave steepness, which means that larger waves of shorter period pro-

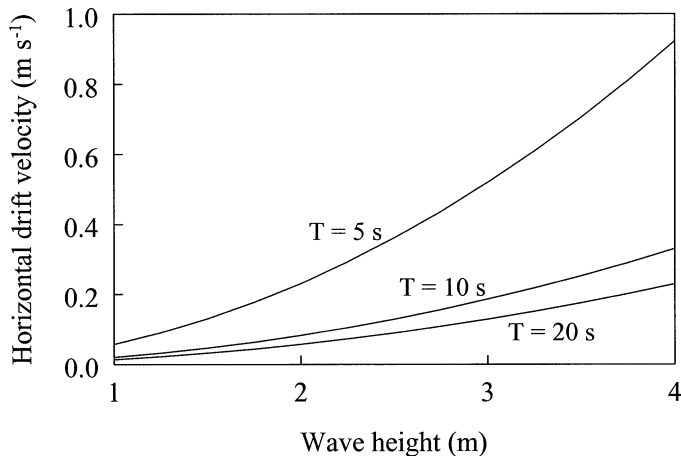


Fig. 5. Magnitude of the horizontal Stokes drift velocity at the water surface, as a function of wave height, for several wave periods,  $T$ . Water depth = 10 m.

duce faster net onshore currents. In some circumstances, these flow speeds are by no means trivial, approaching or even exceeding several centimeters per second. Such flow rates rival those associated with many other important near-shore fluid dynamic processes (e.g., geostrophic currents, buoyancy-induced flows, wind-driven circulation; see Pond and Pickard 1983). As a consequence, it is clear that the net fluid motions from surface gravity waves will potentially have strong biological import.

One arena where Stokes drift appears to influence canopy-forming seaweeds, as alluded to above, is with regard to the forces that act on them. If there is no net mass transport of water, which is the case for purely linear waves, then a strategy of “going with the flow” is often effective at reducing relative velocities and decreasing force. This is particularly true for longer period waves, where applied forces from the oscillations of linear waves are often smaller than the forces that would arise if those same peak orbital flows were applied as unidirectional currents (Fig. 6). This point has been made previously in a number of studies (Koehl 1984, 1986, 1999; Johnson and Koehl 1994; Denny et al. 1997; Gaylord and Denny 1997). The presence of Stokes drift, however, appears to offset many of these advantages. As Fig. 7 indicates, forces imposed on a typical mature *Nereocystis* individual by Stokes waves can exceed those imposed by linear waves by over a factor of four, depending on the wave height and period. The effect is particularly exacerbated under larger, longer period waves, exactly the conditions characteristic of storm waves, which are rarely sampled in the field but which indeed damage many plants (Seymour et al. 1989). In contrast, forces from shorter period Stokes waves might actually be lower than those associated with the linear case, although such situations often correspond to the scenario where moving with the fluid has already increased force because of the phenomenon of inertial loading (Fig. 6).

It is in this situation when Stokes waves are present where an alongshore current can come into play. As is indicated in Fig. 8, steady flows that act perpendicular to the axis of wave propagation can often reduce substantially the forces applied by Stokes waves. This effect typically becomes more pro-

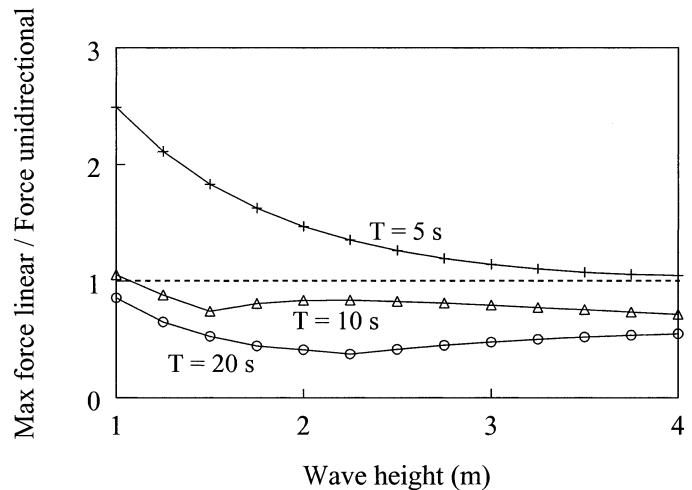


Fig. 6. Ratio of the maximal force applied to a typical *Nereocystis* individual by linear waves to the maximal force from unidirectional flow for a range of wave heights and several wave periods,  $T$ . The unidirectional flows are assumed to have the same speeds as the peak orbital velocities associated with the corresponding waves. Water depth = 10 m, plant length = 10 m.

nounced as the magnitude of the alongshore current increases. With relatively rapid, but nonetheless common, alongshore flow rates of 0.3–0.5 m s<sup>-1</sup> (Figs. 3, 4; see also Gaylord et al. 2002 and references therein), forces can decline by as much as a factor of two. Note that this reduction occurs even though the summed magnitudes of the orbital velocities and alongshore current would otherwise suggest the potential for a much larger total relative velocity.

The general mechanisms by which alongshore currents ameliorate force can be isolated from a careful consideration of the trajectories of plant canopy displacement (Fig. 9). Typically, except under benign conditions where net buoyancy is the largest force, drag dominates the loading (magnitudes of virtual buoyancy and added mass forces vary with

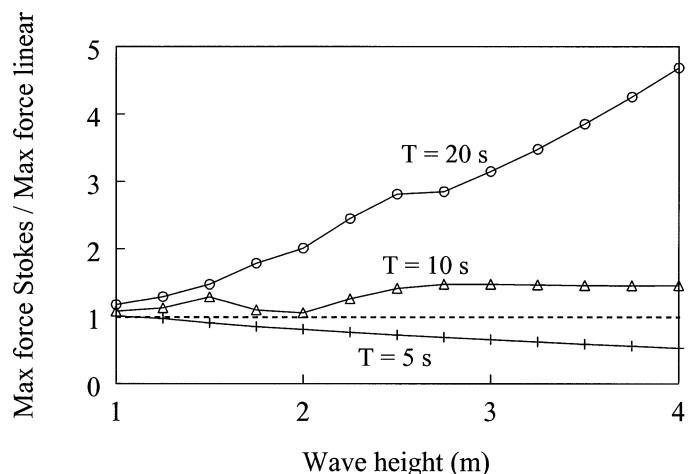


Fig. 7. Ratio of the maximal force applied to a typical *Nereocystis* individual by Stokes waves to the maximal force from linear waves for a range of wave heights and several wave periods,  $T$ . Water depth = 10 m, plant length = 10 m.

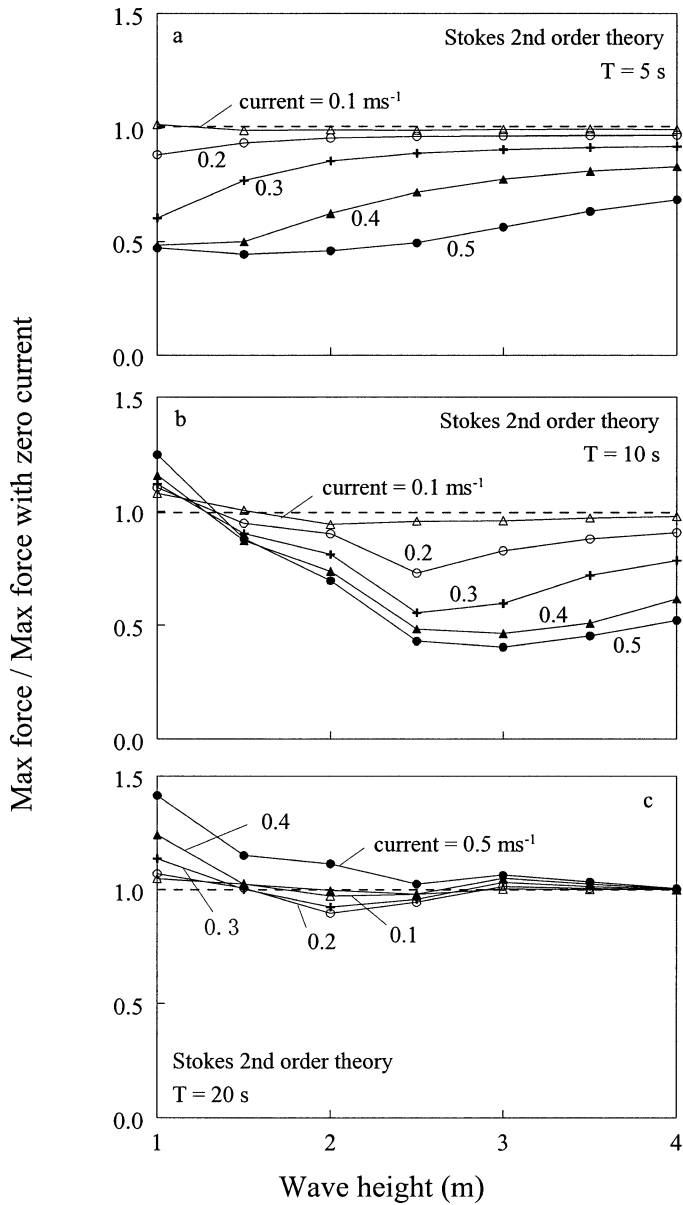


Fig. 8. Ratio of the maximal force applied to a typical *Nereocystis* individual by Stokes waves in the presence of an alongshore current to the maximal force arising in the absence of a current, for a range of wave heights. Water depth = 10 m, plant length = 10 m. (a) Wave period = 5 s. (b) Wave period = 10 s. (c) Wave period = 20 s.

wave conditions and the precise pattern of movement but are almost always minor components). However, in the presence of linear waves, only the vertical component of drag is important because plants are essentially never pulled taut horizontally (Fig. 9a–c). In contrast, kelp individuals exposed to Stokes waves are indeed pulled taut horizontally, making both the vertical and horizontal components of wave-induced drag important, and the resultant total force much larger. The effect of an alongshore current, then, is to reduce both the vertical and horizontal components of wave-induced drag simultaneously at the expense of a modest increase in the

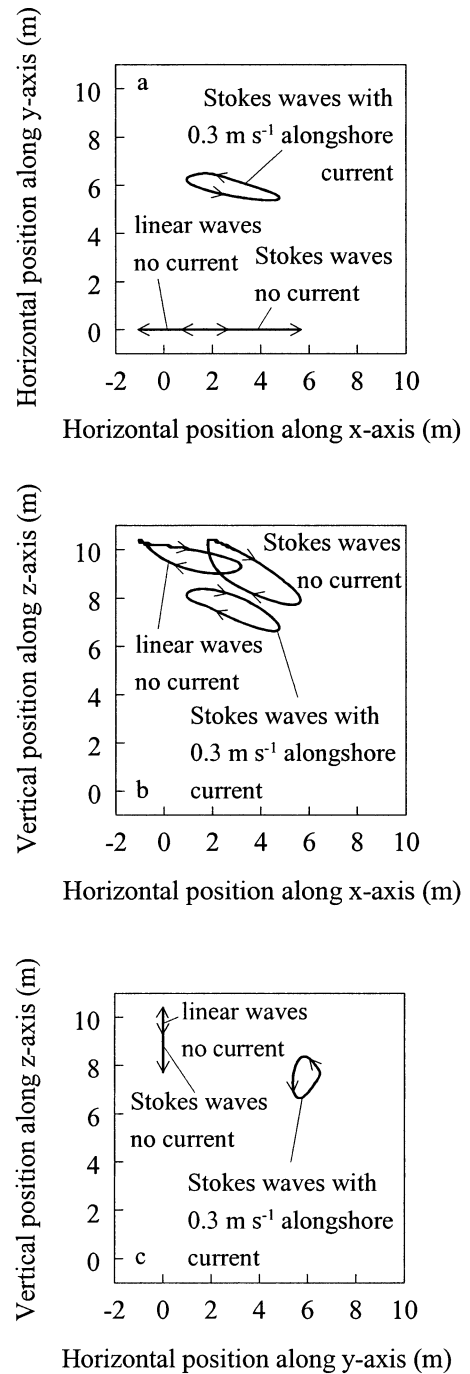


Fig. 9. Predicted trajectories of a typical *Nereocystis* canopy exposed to linear or Stokes waves of 2.5 m height and 10 s period, with or without a  $0.3 \text{ m s}^{-1}$  alongshore current. Notice that the presence of the current reduces the peak displacements (and thereby the stretch in the stipe) along the  $x$ - and  $z$ -axis, the two dominant directions in which drag is applied. The two-headed arrows in panels a and c indicate orbital motion in the vertical plane oriented parallel to the direction of wave propagation. (a) Trajectories viewed from above. (b) Trajectories viewed as if looking along the wave crests. (c) Trajectories viewed as if looking back along the axis of wave propagation. Water depth = 10 m, plant length = 10 m.

alongshore component of force. This is possible because current velocities are typically smaller than wave-induced orbital velocities. The critical force amelioration therefore occurs as the kelp's canopy is pushed off to one side by the current (Fig. 9c), where it lies both lower in the water column (reducing the degree to which the plant's stipe is stretched vertically by the waves; Fig. 9b,c) and closer to its neutral position along the  $x$ -axis (reducing the extent to which the kelp is tugged by waves along the direction of wave propagation; Fig. 9a,b).

This basic phenomenon occurs across a variety of wave-current combinations, with reductions in force especially apparent in the case of shorter or intermediate-period waves (5 and 10 s; Fig. 8a,b). For waves of 20 s period, alongshore currents affect force much less strongly, and under some circumstances (i.e., smaller waves, faster currents) can actually increase force somewhat (Fig. 8c). This less typical outcome arises as a consequence of a kelp canopy now having sufficient time during the longer wave period to swing completely around from its neutral position off to one side, to where it can be fully extended along the axis of wave propagation. In such situations, the alongshore current loses its ability to offset the  $x$ -directed force and thus simply adds to the overall force total. In general, effects of alongshore currents appear to be greatest with smaller wave heights for wave periods of 5 and 20 s and with larger  $H$  for waves of a period of 10 s (Fig. 8). As is indicated in Fig. 4, shorter and longer period wave events in central California are indeed often characterized by smaller wave amplitudes, and the majority of large wave events are often characterized by wave periods between 10 and 16 s.

Such comparisons can also be extended to examine whether, in the face of Stokes drift, alongshore currents intrinsically improve a plant's ability to oscillate passively with the fluid to avoid peak relative flows. This is analogous to the phenomenon explored in Fig. 6 for linear waves and no alongshore current. Data in Fig. 10 suggest that, even when Stokes drift is present, faster alongshore currents allow commonly for a robust drop in force relative to values that would arise in equivalent unidirectional flows (i.e., unidirectional flows with speeds equal to the peak wave velocities), where water motion relative to a plant is unavoidable. This is particularly the case for smaller waves of shorter period ( $H < 2$  m,  $T = 5$  s), where forces from Stokes waves in the absence of an alongshore current would be substantially larger than those that would arise in equivalent unidirectional flows (Fig. 10a). For longer period waves ( $T = 20$  s), the effect of alongshore current speed is negligible and forces in oscillatory flow are universally less than those in unidirectional flow (Fig. 10c). Together, these patterns suggest that, regardless of wave conditions, the action of a sufficiently fast alongshore current can function to offset almost entirely the potential negative consequences of acquiring momentum. The final component of this conclusion is further supported by results of Fig. 11, which show canopy accelerations of kelps exposed to Stokes waves ( $H = 2.5$  m,  $T = 10$  s) with and without an alongshore current. The much smaller accelerations in the presence of the alongshore current indicate a greatly reduced susceptibility to inertial forces.

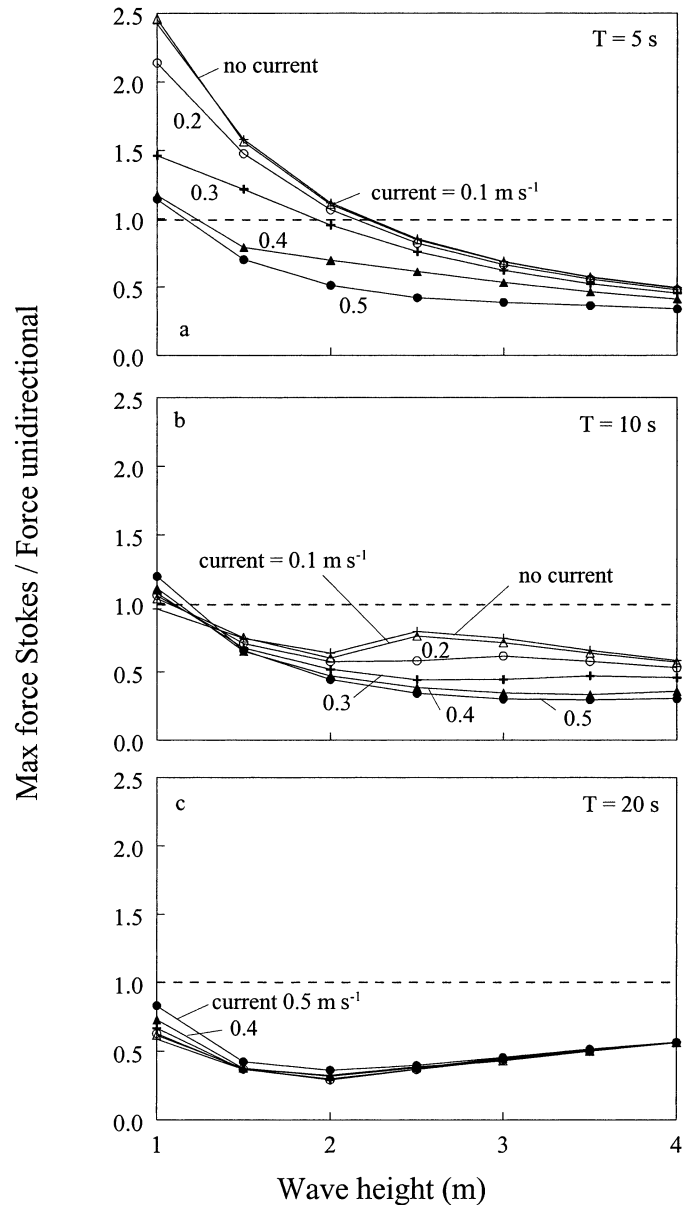


Fig. 10. Ratio of the maximal force applied to a typical *Nereocystis* individual by Stokes waves with or without an alongshore current to the maximal force from unidirectional flow for a range of wave heights. The unidirectional flows are assumed to have the same speeds as the peak orbital velocities associated with the corresponding waves. Water depth = 10 m, plant length = 10 m. (a) Wave period = 5 s. (b) Wave period = 10 s. (c) Wave period = 20 s.

Passive movement in response to flow also has consequences for levels of damping experienced by waves passing through kelp forests. Under all wave and current conditions examined in this study, the kelp's motion reduces the rate at which wave energy is lost to drag, relative to the rate of energy loss that would arise if the plants were stationary (Fig. 12). In most cases, predicted rates of energy loss are 2–20 times lower than they would be for rigid organisms. For waves of shorter period ( $T = 5$  s; Fig. 12a), this ratio

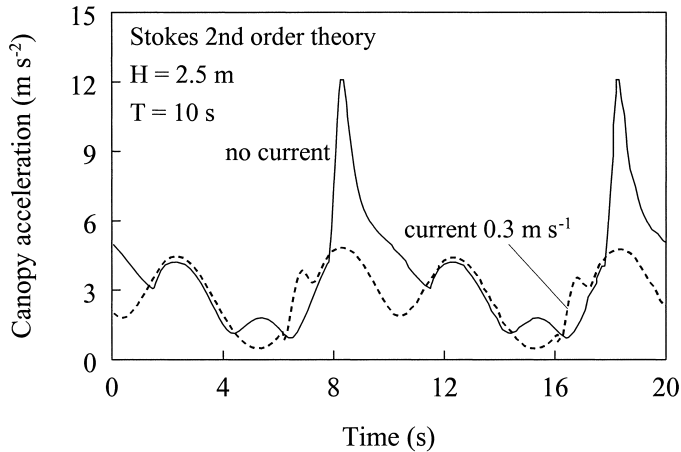


Fig. 11. Acceleration of a typical *Nereocystis* canopy exposed to 2.5-m-high Stokes waves with a 10-s period in the presence or absence of an alongshore  $0.3 \text{ m s}^{-1}$  current. Note the much greater accelerations in the absence of the current, indicating an exacerbated vulnerability to inertial forces.

declines with increasing wave height. In contrast, for longer period waves ( $T = 20 \text{ s}$ ; Fig. 12c), this ratio increases with increasing wave height. For all wave periods and wave heights, faster currents lead to smaller ratios of predicted rates of energy loss relative to those for rigid plants.

Regardless of the presence or magnitude of an alongshore current, however, the degree of damping of surface gravity waves by canopy-forming kelps is low (currents, in contrast, including those generated by coastally trapped waves, can be damped considerably; Jackson and Winant 1983; Jackson 1988, 1998). This fact becomes clear when comparing rates of energy loss from drag to the flux of energy associated with the passage of a wave train through a kelp bed. The energy flux (i.e., the rate of energy transported through a vertical plane of unit width) for a monochromatic train of Stokes waves is given by (Sarpkaya and Isaacson 1981)

$$P_{\text{flux}} = \frac{1}{16} \rho g H^2 C \left( 1 + \frac{2kd}{\sinh(2kd)} \right) \quad (12)$$

If it is assumed that each meter-wide stretch of wave crest must traverse 50 plants on its way through a typical kelp bed (and if the cross-shore width of the bed is not so large that multiple wave crests are within the bed at once—a reasonable approximation for most moderately sized stands and the wave conditions examined in this study), then the ratio ( $50 P_{\text{loss}}/P_{\text{flux}}$ ) provides a rough estimate of the fraction of incident wave energy lost during the wave's propagation through the bed. As Fig. 13 demonstrates, this ratio is predicted to be universally low, in accordance with recent empirical findings (e.g., Elwany et al. 1995). Figure 13 also provides, however, hints of subtler trends across wave conditions and alongshore flow rate. For example, although faster alongshore currents appear to nearly always decrease levels of wave damping, larger waves are predicted to be damped less than smaller waves at shorter periods ( $T = 5 \text{ s}$ ), but more than smaller waves at longer periods ( $T = 20 \text{ s}$ ). Such secondary patterns, while likely moot in many cases

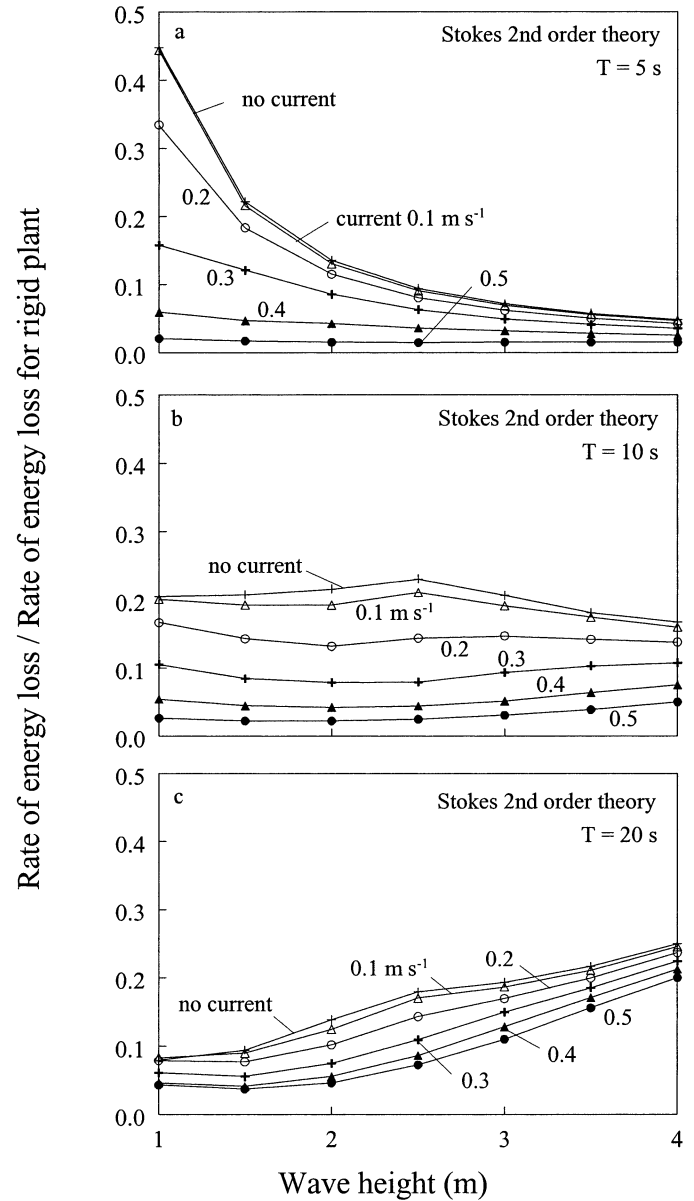


Fig. 12. Ratio of the rate of wave energy loss from a single *Nereocystis*, to the rate of energy loss that would arise if the plant didn't move (aside from passively streamlining) in response to the passing waves, as a function of wave height and alongshore current speed. (a) Wave period = 5 s. (b) Wave period = 10 s. (c) Wave period = 20 s.

involving smaller kelp beds, could become important when waves propagate across exceptionally large and dense stands of macroalgae, where overall levels of damping could conceivably become nontrivial.

#### Implications for kelp canopies

Results of this study therefore provide data on two general fronts. First, evidence presented here indicates that alongshore currents provide a robust mechanism for ameliorating forces imposed on canopy-forming kelps across a wide va-

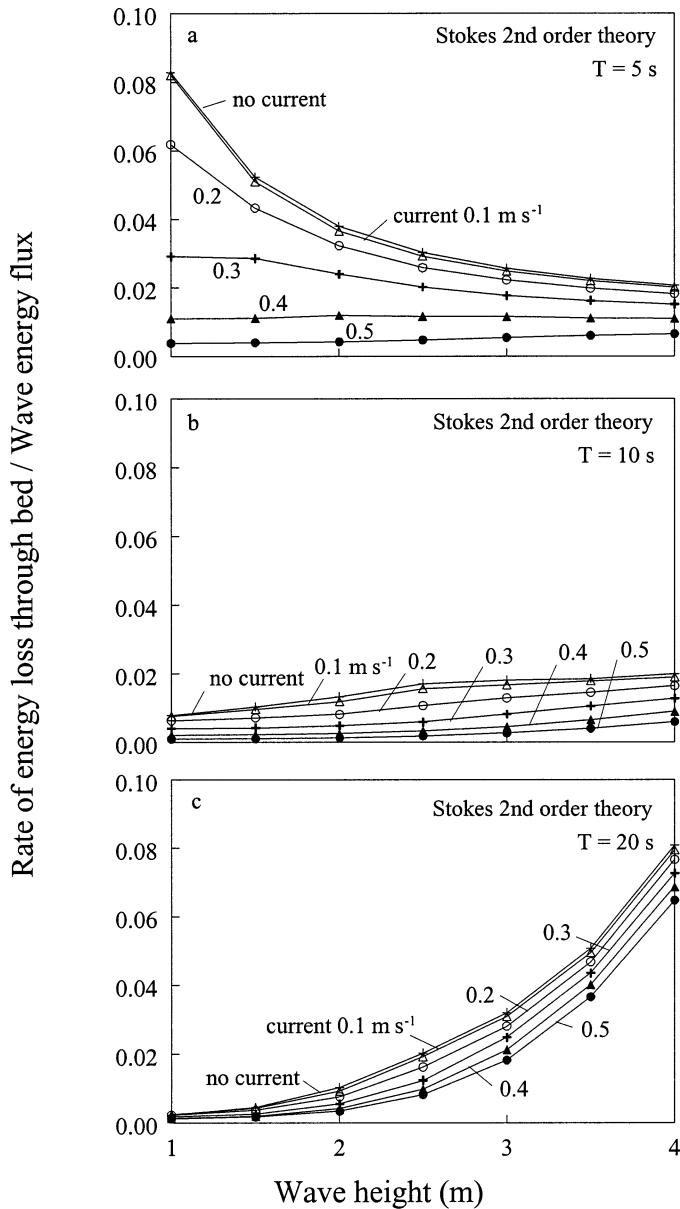


Fig. 13. Ratio of the rate of wave energy loss during wave propagation through a *Nereocystis* bed relative to the incident wave energy flux, as a function of wave height and current speed. Each wave is assumed to propagate through 50 plants on its way to the shore. (a) Wave period = 5 s. (b) Wave period = 10 s. (c) Wave period = 20 s.

riety of incident wave conditions. Second, this study yields insight into how plants in turn influence the waves themselves through hydrodynamic feedback. Although such core model findings should be applied in their strictest sense only to *Nereocystis*, major themes might also repeat in other canopy-forming species as well. *Pelagophycus*, for example, maintains its blades near the water surface like *Nereocystis*, and probably responds similarly to flow. *Macrocystis* produces a cluster of fronds that extend throughout the entire water column and thus shows a somewhat different vertical architecture. However, as much as 70–80% of the biomass

of individuals of this species can be held within the canopy (D. C. Reed unpubl. data), which suggests in turn that flow-induced motion of *Macrocystis* could be more similar to that of *Nereocystis* than might initially be expected. Additionally, although previous studies (e.g., Jackson and Winant 1983; Jackson 1998) have emphasized the exceptionally slow flows present within extensive *Macrocystis* forests in Southern California—which would suggest only a minor role for currents in affecting the motion of these organisms—beds of *Macrocystis* elsewhere are universally far smaller and could therefore damp currents much less. Thus, speeds of currents past *Macrocystis* plants in many locations along the coast of North America might be of sufficient magnitude to have effects similar to those predicted for *Nereocystis*. Until the necessary experiments have been conducted, however, such possibilities will remain in the realm of speculation.

Much of the work described here builds on previous models (e.g., Seymour and Hanes 1979; Dalrymple et al. 1984; Seymour 1996) in accounting explicitly for particular morphological features and dynamical behaviors (i.e., streamlining, acquisition of momentum, reorientation) that characterize canopy-forming kelps and control their mechanics of motion. The present work also complements recent studies on smaller, submergent macroalgae (e.g., *Laminaria hyperborea*) that exhibit somewhat different responses to flow (Asano et al. 1992; Kobayashi et al. 1993; Dubi and Torum 1994). As such, although it should be emphasized that the results presented above have not attempted to examine the full range of possible flow conditions and kelp sizes/shapes and have ignored complexities such as interactions among multiple individuals within dense kelp stands, this research brings us yet one step closer to a full understanding of how seaweeds in general and canopy-forming kelps in particular survive successfully in their fluid environments as they cope with the omnipresent waves that impinge on them. Of course, the topic of wave forces represents but one of a whole suite of factors influencing the population dynamics of these plants and their ecosystem functioning; clearly a full synthesis will require consideration not only of processes driving physical disturbance, but of all such factors.

## References

- ABBOTT, I. A., AND G. J. HOLLENBERG. 1976. Marine algae of California. Stanford Univ. Press.
- ASANO, T., H. DEGUCHI, AND N. KOBAYASHI. 1992. Interaction between water waves and vegetation, p. 2710–2723. *In* Proceedings of the 23rd International Conference on Coastal Engineering. American Society of Civil Engineers.
- BACON, S., AND D. J. T. CARTER. 1991. Wave climate changes in the North-Atlantic and North Sea. *Int. J. Climatol.* **11**: 545–558.
- BATCHELOR, G. K. 1967. An introduction to fluid dynamics. Cambridge Univ. Press.
- DALRYMPLE, R. A., J. T. KIRBY, AND P. A. HWANG. 1984. Wave diffraction due to areas of energy dissipation. *J. Waterw. Port Coast. Ocean Eng.* **110**: 67–79.
- DAYTON, P. K., V. CURRIE, T. GERRODETTE, B. D. KELLER, R. ROSENTHAL, AND D. VENTRESCA. 1984. Patch dynamics and stability of some California kelp communities. *Ecol. Monogr.* **54**: 253–289.
- , M. J. TEGNER, P. E. PARNELL, AND P. B. EDWARDS. 1992.

- Temporal and spatial patterns of disturbance and recovery in a kelp forest community. *Ecol. Monogr.* **62**: 421–445.
- DENNY, M. W. 1988. Biology and the mechanics of the wave-swept environment. Princeton Univ. Press.
- . 1995. Predicting physical disturbance: Mechanistic approaches to the study of survivorship on wave-swept shores. *Ecol. Monogr.* **65**: 371–418.
- , AND B. GAYLORD. 2002. The mechanics of wave-swept macroalgae. *J. Exp. Biol.* **205**: 1355–1362.
- , AND E. A. COWEN. 1997. Flow and flexibility II. The roles of size and shape in determining wave forces on the bull kelp *Nereocystis luetkeana*. *J. Exp. Biol.* **200**: 3165–3183.
- , B. HELMUTH, AND T. DANIEL. 1998. The menace of momentum: Dynamic forces on flexible organisms. *Limnol. Oceanogr.* **43**: 955–968.
- DUBI, A., AND A. TORUM. 1994. Wave damping by kelp vegetation, p. 142–156. *In* Proceedings of the 24th International Conference on Coastal Engineering. American Society of Civil Engineers.
- ELWANY, M. H. S., W. C. O'REILLY, R. T. GUZA, AND R. E. FLICK. 1995. Effects of Southern California kelp beds on waves. *J. Waterw. Port Coast. Ocean Eng.* **121**: 143–150.
- FOSTER, M. S., AND D. R. SCHIEL. 1985. The ecology of giant kelp forests in California: A community profile. U.S. Fish and Wildlife Service, Biological Report 85.
- GAYLORD, B. 2000. Biological implications of surf-zone flow complexity. *Limnol. Oceanogr.* **45**: 174–188.
- , AND M. W. DENNY. 1997. Flow and flexibility I. Effects of size, shape, and stiffness in determining wave forces on the stipitate kelps *Eisenia arborea* and *Pterygophora californica*. *J. Exp. Biol.* **200**: 3141–3164.
- , C. A. BLANCHETTE, AND M. W. DENNY. 1994. Mechanical consequences of size in wave-swept algae. *Ecol. Monogr.* **64**: 287–313.
- , B. B. HALE, AND M. W. DENNY. 2001. Consequences of transient fluid forces for compliant benthic organisms. *J. Exp. Biol.* **204**: 1347–1360.
- , D. C. REED, P. T. RAIMONDI, L. WASHBURN, AND S. R. MCLEAN. 2002. A physically based model of macroalgal spore dispersal in the wave and current-dominated nearshore. *Ecology* **83**: 1239–1251.
- GREVEMEYER, I., R. HERBER, AND H. H. ESSEN. 2000. Microseismological evidence for a changing wave climate in the north-east Atlantic Ocean. *Nature* **408**: 349–352.
- JACKSON, G. A. 1988. Kelvin wave propagation in a high drag coastal environment. *J. Phys. Oceanogr.* **18**: 1733–1743.
- . 1998. Currents in the high drag environment of a coastal kelp stand off California. *Cont. Shelf Res.* **17**: 1913–1928.
- , AND C. D. WINANT. 1983. Effect of a kelp forest on coastal currents. *Cont. Shelf Res.* **2**: 75–80.
- JOHNSON, A. S., AND M. A. R. KOEHL. 1994. Maintenance of dynamic strain similarity and environmental stress factor in different flow habitats: Thallus allometry and material properties of a giant kelp. *J. Exp. Biol.* **195**: 381–410.
- KINSMAN, B. 1965. Wind waves. Prentice-Hall.
- KOBAYASHI, N., A. W. RAICHLE, AND T. ASANO. 1993. Wave attenuation by vegetation. *J. Waterw. Port Coast. Ocean Eng.* **119**: 30–48.
- KOEHL, M. A. R. 1984. How do benthic organisms withstand moving water? *Am. Zool.* **24**: 57–70.
- . 1986. Seaweeds in moving water: Form and mechanical function. *In* T. J. Givnish [ed.], *On the economy of plant form and function*. Cambridge Univ. Press.
- . 1999. Ecological biomechanics of benthic organisms: Life history, mechanical design and temporal patterns of mechanical stress. *J. Exp. Biol.* **202**: 3469–3476.
- , AND R. S. ALBERTE. 1988. Flow, flapping, and photosynthesis of *Nereocystis luetkeana*: A functional comparison of undulate and flat blade morphologies. *Mar. Biol.* **99**: 435–444.
- , AND S. A. WAINWRIGHT. 1977. Mechanical adaptations of a giant kelp. *Limnol. Oceanogr.* **22**: 1067–1071.
- KOMAR, P. D. 1998. Beach processes and sedimentation, 2nd ed. Prentice-Hall.
- LONGUET-HIGGINS, M. S. 1953. Mass transport in water waves. *Phil. Trans. R. Soc. Lond., Ser. A* **245**: 535–581.
- MENDEZ, F. J., I. J. LOSADA, AND M. A. LOSADA. 1999. Hydrodynamics induced by wind waves in a vegetation field. *J. Geophys. Res.* **104**: 18,383–18,396.
- POND, S., AND G. L. PICKARD. 1983. *Introductory dynamical oceanography*, 2nd ed. Pergamon.
- PRESS, W. H., S. A. TEUKOLSKY, W. T. VETTERLING, AND B. P. FLANNERY. 1992. *Numerical recipes*. Cambridge Univ. Press.
- SARPKAYA, T., AND M. ISAACSON. 1981. *Mechanics of wave forces on offshore structures*. Van Nostrand Reinhold.
- SCHLICHTING, H. 1979. *Boundary-layer theory*, 7th ed. McGraw-Hill.
- SEYMOUR, R. J. 1996. Effects of Southern California kelp beds on waves—discussion. *J. Waterw. Port Coast. Ocean Eng.* **122**: 207–208.
- , AND D. M. HANES. 1979. Performance analysis of tethered float breakwater. *J. Waterw. Port. Coast. Ocean Eng.* **105**: 265–280.
- , M. J. TEGNER, P. K. DAYTON, AND P. E. PARNELL. 1989. Storm wave induced mortality of giant kelp, *Macrocystis pyrifera*, in Southern California. *Estuar. Coast. Shelf Sci.* **28**: 277–292.
- STEVENS, C. L., C. L. HURD, AND M. J. SMITH. 2001. Water motion relative to subtidal kelp fronds. *Limnol. Oceanogr.* **46**: 668–678.
- UTTER, B. D., AND M. W. DENNY. 1996. Wave-induced forces on the giant kelp *Macrocystis pyrifera* (Agardh): Field test of a computational model. *J. Exp. Biol.* **199**: 2645–2654.

Received: 18 September 2002

Accepted: 25 October 2002

Amended: 21 November 2002